

Memory augment is All You Need for image restoration

Xiaofeng Zhang, *Student Member, IEEE*, Chao Chen Gu*, *Member, IEEE*, Shan Ying Zhu, *Member, IEEE*,

Abstract—Image restoration is a low-level vision task, most CNN methods are designed as a black box, lacking transparency and internal aesthetics. Although some methods combining traditional optimization algorithms with DNNs have been proposed, they all have some limitations. In this paper, we propose a three-granularity memory layer and contrast learning named MemoryNet, specifically, dividing the samples into positive, negative, and actual three samples for contrastive learning, where the memory layer is able to preserve the deep features of the image and the contrastive learning converges the learned features to balance. Experiments on Derain/Deshadow/Deblur task demonstrate that these methods are effective in improving restoration performance. In addition, this paper’s model obtains significant PSNR, SSIM gain on three datasets with different degradation types, which is a strong proof that the recovered images are perceptually realistic. The source code of MemoryNet can be obtained from <https://github.com/zhangbaijin/MemoryNet>

Index Terms—Image restoration, shadow removal, rain removal, image deblur

I. INTRODUCTION

Image restoration is a low-level vision task, it refers to the recovery of degraded images. Common types of degradation include additional noise, blur and so on. The quick advancement of computer vision in recent years has made it possible to handle an increasing number of degradation tasks, including super-resolution, single-image defogging, image de-shadowing, and image rain removal.

Image restoration which is a highly discomfoting problem because there exist infinite number of feasible solutions. Image prior is used [1]–[7] to restrict the solution space to valid/natural images. However, designing such a prior is a challenging task and often cannot be generalized. To improve this problem, recent state-of-the-art methods [8]–[16] employ convolutional neural networks (CNNs) to learn more general prior large-scale data statistics implicitly by capturing natural images. The model design of the CNN-based method is primarily responsible for its performance improvement over the others. With the success of generative adversarial networks, some generative models for distorted image restoration have been introduced such as image inpainting [17]–[21], image shadow removal [22] image rain removal [26], [28], and image cloud removal [27]. Take an example of image de-shadowing, these methods formulate the distortion restoration problem as

finding the appropriate warping and predicting the dense grid, which achieve the state-of-the-art results. However, existing efforts mainly focus on the model structure, one opportunity that is widely ignored is memory learning approach.

We believe there are two issues with the image restoration research: first, when the model converges, a limitation problem has been exposed: the performance cannot be improved significantly and the model remains saturated at this time. Unexpectedly, such limitations cannot be tackled by simply adding more layers. In fact, when training dataset is given, its distribution is objective and fixed. Unexpectedly, such limitations cannot be tackled by simply adding more layers. Therefore, how to make the network learn more potential information while keeping the original underlying network unchanged is a very difficult problem to solve. Second, shadow removal unlike image inpainting, where an entire area is white shaded, it must perform certain operations on the semi-dark area while retaining the original image features, which is difficult to achieve because you need to take into account the real image information under the shaded area.

Therefore, we designed MemoryNet, which is specifically divided into memory augment and contrastive learning. On the one hand, to solve the first problem aboved mentioned, this paper introduces a novel memory augment module, MA (memory augment) additionally models a learnable latent attribute variable to remember prototypical patterns of representative structures in a global range that generally covers a diverse sample of identities. The model’s confidence for unseen classes is increased by increasing this memory likelihood by the prediction. MA also conveys additional domain-level low-frequency information learned from previously viewed samples for collaborative decision making, avoiding GAP-like semantic abstraction. For more details, we re-collect features into a predefined coarse-to-fine prototype index by reading memory for further similarity measures. Unlike searching for relevant discriminative regions in two images, this prototype alignment is lightweight and similar to a multi-level hash. The memory augment network adds well to the application effect of image de-shadowing, which proves its usefulness inside the ablation study. On the other hand, to solve the second problem mentioned, we design a contrast learning network with weakly supervised learning as shown in Fig.2. We define the image de-shadowing task as a three-class classification problem, corresponding to positive (clean samples), standard (de-shadowed samples), and negative samples (shadowed samples), with global features as anchor points, to enable the model to discriminate whether the global features and local features come from the same image. As a result, contrastive

Xiao Feng Zhang, Chao Chen Gu and Shan Ying Zhu are with Center for Intelligent Wireless Network and Collaborative Control, Shanghai Jiao Tong University, Shanghai, China. (email:framebreak@sjtu.edu.cn; jacygu@sjtu.edu.cn; shyzhu@sjtu.edu.cn)

Manuscript received August 18, 2022

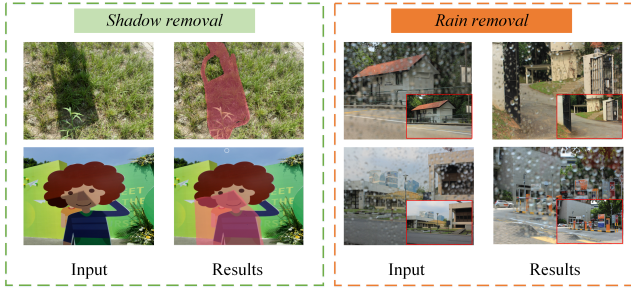


Fig. 1. Results of MemoryNet’s image shadow removal and image deraining

learning constrains the anchored image to a closed image by contrast learning the upper and lower boundaries, which helps the restoration network approach the positive image while avoiding the negative image.

We have conducted a lot of experiments on three tasks: image de-shadowing/image de-raining/image de-blurring, all with satisfactory results. The results of this paper are shown in Fig 1, in summary. The main contributions of this work are:

- 1) In this paper, a novel end-to-end network named MemoryNet is designed for image restoration, which generates context-rich and spatially accurate outputs.
- 2) In this paper, we design a novel memory augment layer, which models a learnable latent property variable to remember globally representative structural prototype patterns.
- 3) We carry out extensive experiments on three typical image restoration tasks, i.e., synthetic image de-shadow, real image deraining, and image deblurring, showing that our proposed MemoryNet achieves great results while maintaining an attractive computational complexity. In addition, we provide detailed ablation studies, qualitative results and generalization tests.

II. RELATED WORK

A. Image shadow removal

supervised shadow removal While this paper’s major contribution is to suggest a dataset SRD, the earliest weakly supervised first for DshadowNet [23] has the biggest feature of fully automatic end-to-end implementation of shadow removal (A New Dataset for Shadow Removal). With the purpose of jointly utilizing the benefits of one another’s advancements, ST-CGAN [22] provide a multitasking perspective that varies from all other existing approaches in that it learns detection and elimination together in an end-to-end manner. By estimating a linear transformation function, SID and DSC [38], [39] create depth networks to illuminate the shaded areas. for shadow (half-shadow). A broad framework is created by RSI-GAN [40], to mine illumination and residual data using multiple GANs for shadow removal. DHAN [41] uses a dual-level aggregation network (DHAN) in order to eliminate boundary artifacts. Auto-exposure [42], [44] aims to mine the contextual information of the shadowed and non-shadowed regions.

Weakly supervised shadow removal According to Mask-shadowGAN [43] prior deep learning approaches to shadow

removal challenges are supervised, paired data. However, getting the matched dataset can be a challenge. According to LG-shadow [46] in actual practice, CNN training favors unpaired data since it is simpler to train on. The Transformer network based on the attention mechanism is suggested by SpA-Former [50] to learn the shaded spatial attention graph alongside Transformer.

Unsupervised learning shadow removal

G2R [48] took use of the fact that shaded photographs frequently have both shaded and un-shaded areas. By using this technique, it is possible to crop a collection of shaded and unshaded patches to provide unpaired data for network training, offering the possibility of three sub-network modules: shadow production, shadow removal, and shadow refining. The shadow removal task is carried out by TC-GAN [49] in an unsupervised manner. contrasting the cyclic consistency-based bidirectional mapping method with the GAN-based unsupervised shadow removal approach.

B. Image rain removal

supervised rain removal

The attention mechanism is introduced in the generator and discriminator by SPANet [28], which also generates an attention map over a number of time steps and identifies the area in the original graph that the network has to pay attention to: the rain point and its surroundings. The encoder-decoder architecture of NEDNet [29] cites non-local enhancement, which successfully removes rain of varying densities while perfectly maintaining image details. Yang [30] proposes a new pipeline: to complete the de-raining, first detect the location of the rain, then estimate the rain line, and lastly remove the background layer. Ren [31] provide a starting point: The model consists of six stages, each of which is separated into two models and receives as input the stitching of the initial rain map and the de-rain map produced in the step before it.

Semi-supervised rain removal Wei and Huang [32], [33] propose semi-supervised models that can record different rain degradation prototypes and update them by self-supervised learning.

Un-supervised rain removal Guo [34] propose unsupervised attention mechanism-guided rain extraction model E. They use the attention mechanism for the spatial domain of both rain and no-rain maps, and use a CycleGAN loop structure with two constrained branches to de-rain.

C. The development of memory module

Dong Gong [53] is the first to introduce memory module to anomaly detection task, which considers Encoder can be regarded as query generator; Decoder input is the new feature maps of size (H,W,C) generated by Memory module, which is used to reconstruct the generated images, which can be interpreted as reconstructing Encoder feature maps, and the generated new feature maps contain more information about normal frames, which makes Decoder reconstruct the anomalous frames to get a larger reconstruction error after reconstruction. Park [54] core idea is to enrich the normal frame information in Auto Encoder to better distinguish normal

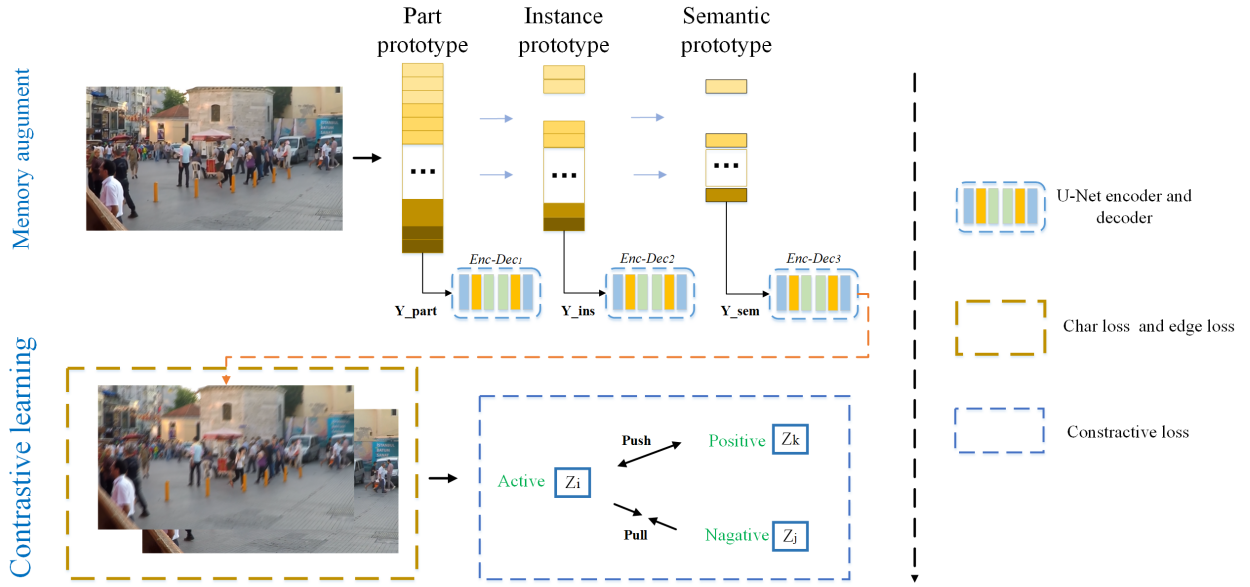


Fig. 2. The structure of MemoryNet, it is divided into memory augment network and contrastive learning.

frames from abnormal frames during testing and to achieve the purpose of video abnormality detection. MMOS [62] is a de-rain task, and they believe that the most important link is the intermediate Memory module used to model/store the different rain patterns for the rain degradation process. Specifically, $z(x)$ is equivalent to a query to find the most relevant items in the memory and combine them with soft-attention as a guide for the rain removal task. Chen F [55] is a part of the memory module to the task of pedestrian re-identification.

III. NETWORK STRUCTURE

MemoryNet is inspired by [51]–[54], as shown in Fig. 2. The network is mainly composed of two parts. The first part is memory augment, which is composed of two encoder and decoder network followed by the residual network. This paper uses a coder-decoder to learn multi-scale contextual information, while the final stage operates on the original image resolution to preserve fine spatial details. The second part is contrastive learning network.

Instead of simply cascading multiple stages, we add a supervised attention module between each two stages. Under the supervision of the real image, our module readjusts the feature maps of the previous stage before passing them on to the next stage. In addition, we introduce a cross-stage feature fusion mechanism in which the intermediate multiscale contextual features of the earlier subnetworks help consolidate the intermediate features of the latter subnetworks.

A. Memory augment

1) **How to detect abnormal area?:** We refer blur as a kind of abnormal pattern, thus we should detect where is abnormal and refine the abnormal as normal. In this intuition, we combine abnormal detection and completion proxy. This baseline is feasible for transformer framework. Here, we define shadow img as abnormal and clean img as normal. We

follow traditional Encoder and Decoder structure of abnormal detection which first sent clean img to memory-augmented encoder/decoder to record normal pattern. You can follow [56] to conduct such structure. You do not need to change the basic encoder/decoder of your original framework, just insert the memory and supervision in it. After training this abnormal detection phase, the encoder and decoder meet reconstruction capability while the memory records normal pattern. When we sent a blur img, this model is unable to recover it to clean.

2) **How to transfer abnormal to normal?:** The basic idea is similar to Context Encoder/Decoder, since we refer the de-shadow as a proxy task similar to completion. In Training phase, we already know the encoder is weak in de-shadow, since we train it only with clean imgs. Thus we introduce a latent contextual regressor to recover the blur area.

3) **Memory augment:** The structure of Memory augment is shown in Fig. 3. The reconstruction error is nevertheless minimal when the input is an irregular frame due to the high characterisation ability of the CNN model, which causes the outcome to be erroneous. This issue is resolved by the addition of the Memory Module to Encoder and Decoder, which enables Encoder and Decoder to record the normal frame properties and weakens CNN's capacity for characterisation in order to discriminate between normal and abnormal frames. In this research, we reformulate the interpretable probability processing of the final CNN layer for the classification-based ranking retrieval. Then, in order to lessen the domain bias, we construct a hierarchical memory adjustment and alignment module.

The memory module contains N prototypes recorded by a metric $M \in \mathbb{R}^{N \times C}$ with a fixed feature dimension C . N is the number of Memory items, a hyperparameter that is adjusted as needed, and memory addressing calculates the weight of each query with respect to all memory items, and then uses an attention-based The attention-based addressing operator for accessing memory, i.e., the memory reader, is then used to

assign each image to the alternate prototype:

$$w_{ij} = \frac{\exp(d(\mathbf{f}_i, \mathbf{m}_j))}{\sum_{j=1}^N \exp(d(\mathbf{f}_i, \mathbf{m}_j))}, \quad (1)$$

$$d(\mathbf{f}_i, \mathbf{m}_j) = \frac{\mathbf{f}_i \mathbf{m}_j^\top}{\|\mathbf{f}_i\| \|\mathbf{m}_j\|},$$

where f_i and m_j are the feature and prototype slice prototype metric M from input f . w_{ij} is the normalized weight to measure the cosine similarity $d(-, -)$ between f_i and m_j . Therefore, the assigned prototype from feature f can be calculated h as:

$$y = \text{Memory}(\mathbf{f}, M) = \sum_{i=1}^{H \times W} \sum_{j=1}^N w_{ij} \mathbf{m}_j \quad (2)$$

We construct the memory augment shown in Fig. 2. The MA(memory augment) consists of hierarchical semantics composed of a prototype M , i.e., partial instance semantics, to avoid over-abstraction. The instance and semantic prototypes are summarized from the previous low-level prototypes. Thus, while spanning various semantic diversities in the memory slots of the prototypes, M is shared to represent all generic concept samples. Specifically, we define the prototype metric M as $2 \times (\mathbf{P} \times \mathbf{I} \times \mathbf{S} \times N_c) \times C$ shape, where P , I and S are each prototype number predefined for the part, instance and semantic levels, respectively, and N_c is the category number. Before summarizing the semantic prototypes, each part and instance prototype is replicated for both modalities. Thus, for internal modal gaps, we keep the individual modalities in the lower level representative modal part and instance prototypes, and then align them jointly at the semantic level. As shown in Figure 2, each higher-level prototype item can be summarizing its lower range. For example, the i_{th} row $m_{ins,i}$ of the instance prototype sub-metric M_{ins} can be viewed as a weighted sub-segment M_{part}

$$\mathbf{m}_{ins,i} = \frac{1}{\mathcal{P} \times \mathcal{S} \times N_c} \sum_{j=(\mathcal{P} \times \mathcal{S} \times N_c) \times (i-1) + 1}^{(\mathcal{P} \times \mathcal{S} \times N_c) \times i} \alpha \cdot \mathbf{m}_{part,j} \quad (3)$$

$$\begin{aligned} y_{part} &= M_{part}(\mathbf{f}, M_{part}) \\ y_{ins} &= M_{ins}(h_{part}, M_{ins}) \\ y_{sem} &= M_{sem}(h_{ins}, M_{sem}) \end{aligned} \quad (4)$$

After training this abnormal detection phase, the encoder and decoder meet reconstruction capability while the memory records normal pattern. When we sent a blur img, this model is unable to recover it to clean. So the input of encode for each stage is:

$$\begin{aligned} \text{Enc1}_{input} &= y_{part} \\ \text{Enc2}_{input} &= y_{ins} + \mathbf{SFe}_{Dec1} \\ \text{Enc3}_{input} &= y_{sem} + \mathbf{SFe}_{Dec2} \end{aligned} \quad (5)$$

where \mathbf{SFe} represent the shallow feature fusion product. Meanwhile, in this stage of memory augment, abnormal features and normal features are reconstructed with constraints, which we call L_{recon} , defined as follow:

$$l_{recon} = \|\text{Mem}(\text{Dec}(\text{Enc}(Y))), Y\|_2 \quad (6)$$

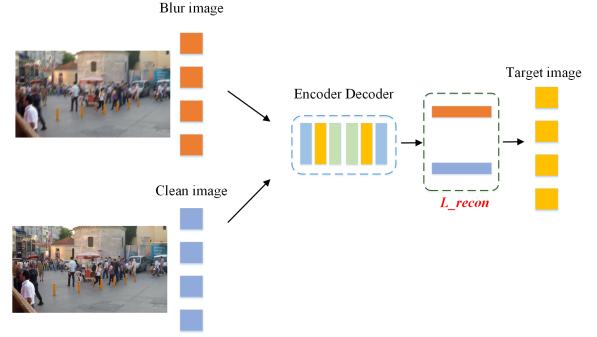


Fig. 3. The structure of memory augment in decoder and encoder

B. Loss Function Design

The following loss function of MemoryNet is:

$$\mathcal{L} = \sum_{S=1}^3 [\mathcal{L}_{char}(\mathbf{X}_S, \mathbf{Y}) + \lambda \mathcal{L}_{edge}(\mathbf{X}_S, \mathbf{Y})] + L_{recon} \quad (7)$$

where Y represents the ground-truth image, and \mathcal{L}_{char} is the Charbonnier loss:

$$\mathcal{L}_{char} = \sqrt{\|\mathbf{X}_S - \mathbf{Y}\|^2 + \varepsilon^2} \quad (8)$$

with constant ε empirically set to 10^3 for all the experiments. In addition, \mathcal{L}_{edge} is the edge loss, defined as:

$$\mathcal{L}_{edge} = \sqrt{\|\Delta(\mathbf{X}_S) - \Delta(\mathbf{Y})\|^2 + \varepsilon^2} \quad (9)$$

IV. EXPERIMENT

Implementation details Our CR-MemoryNet is an end-to-end trainable model that does not require any pre-training. It was implemented using PyTorch 1.8.0 and an NVIDIA GTX 3090 GPU. In this paper, we chose three evaluation metrics, PSNR and SSIM, and RMSE.

Shadow removal The dataset used in this paper is ISTD [22]. We empirically use the Adam optimizer to optimize our network. In our experiments, we set the first momentum value, the second momentum value weights to decay to 0.9, 0.999, and 5×10^{-4} . ISTD comprises of 540 test triples and 1330 training triples of shaded, shaded masked, and unshaded pictures. For training and testing, the SRD contains 2680 and 408 pairs of images, respectively.

Real rain removal We use the DeRainDrop dataset [25] for training and testing. It provides 861 image pairs for training and has two testing datasets (i.e., testA and testB). TestA is a subset of testB, which contains 58 pairs of good aligned images. TestB has 249 image pairs with a small portion of images which are not perfectly aligned.

Image deblurring For image deblurring, similar to [51], [64]–[66], we trained our model with 2,103 image pairs from GoPro [67], unlike the predefined blurring kernel, these two datasets were generated in real scenes involving real-world degradation factors, such as camera response functions and also human consciousness dynamic blurring.

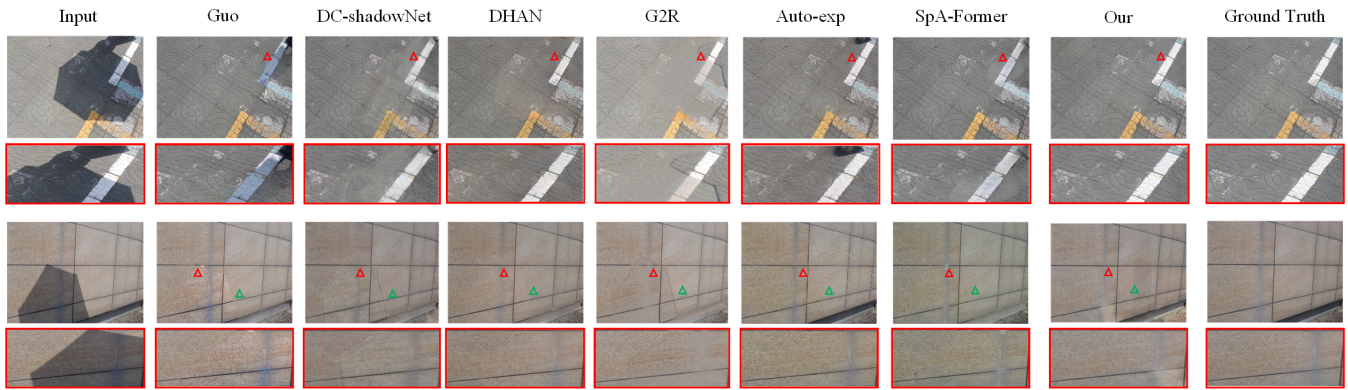


Fig. 4. Visual performance comparison of image deshadow on ISTD dataset



Fig. 5. Visual performance comparison of image deraining on Raindrop dataset

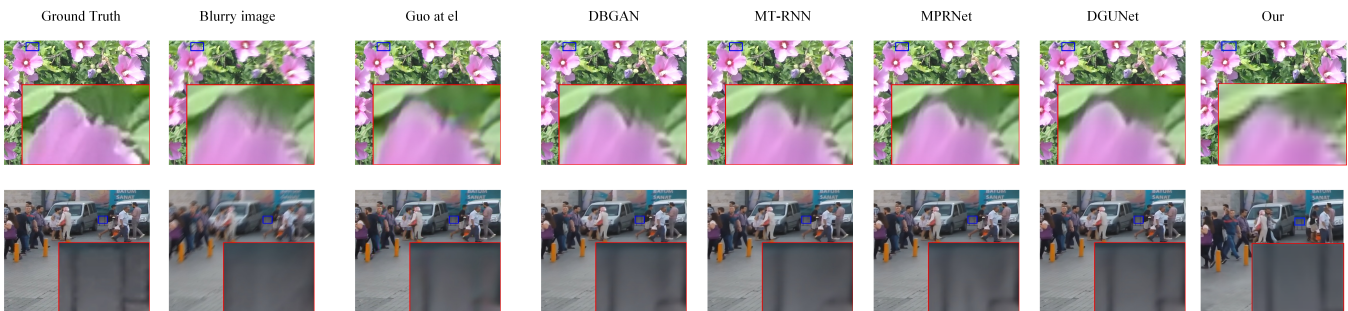


Fig. 6. Visual performance comparison of image deblurring on GOPRO dataset

A. Comparison with State-of-the-Art Methods

1) **Shadow removal:** Our method is compared with existing methods including Yang [37], Guo [35], Gong [36], DeShadowNet [23], STC-GAN [22], DSC [39], Mask-ShadowGAN [43], RIS-GAN [40], DHAN [41], SID [38], LG-shadow [46], G2R [48], DC-ShadowNet [24], Auto-exp [42], SpA-Former [50], CANet [44]. We adopt the root mean square error (RMSE), structure similarity index (SSIM) and Peak Signal to Noise Ratio (PSNR) in the LAB color space as evaluation metrics. Table I report the RMSE, SSIM and PSNR values, respectively, of different shadow removal methods on the ISTD dataset [22]. The quantitative comparison is shown in Fig. 4. MemoryNet achieves the best performance on PSNR whether

it is partially shaded or non-partially shaded, or unshaded region, the RMSE in this paper also achieves the best performance on the unshaded region, surpassing SOTA in general. SID [38] and G2R [48] may incorrectly handle relatively dark non-shaded regions bringing some misestimation. It turns out that their model fails to take full advantage of the shadow mask information, even if their network input contains shadowmask. Auto-exp [42] and CANet [44] use triplet dataset (input, mask, target), which perform well in terms of indicators. But it is necessary to obtain the mask of the shadow in practical application. From the perspective of application, this is of no practical value. The training in this paper only needs pairs of data, and the test only needs a simple shadow graph, which is of great practical significance.

TABLE I
PERFORMANCE COMPARISON OF IMAGE SHADOW REMOVAL ON ISTD. (THE RED MARKED REPRESENTATIVE RANKED FIRST AND THE BLUE MARKED REPRESENTATIVE RANKED SECOND)

Models	RMSE	RMSE-N	RMSE-S	SSIM	SSIM-N	SSIM-S	PSNR	PSNR-N	PSNR-S
<i>Traditional methods</i>									
Yang[TIP2012] [37]	15.63	14.83	19.82	-	-	-	-	-	-
Guo[TPAMI2013] [35]	9.3	7.46	18.95	0.919	0.944	0.978	23.07	24.86	30.98
Gong[BMVC2014] [36]	8.53	7.29	14.98	0.908	0.929	0.98	24.07	25.26	32.43
<i>Supervised learning methods</i>									
DeShadowNet[CVPR2017] [23]	7.83	7.19	12.76	-	-	-	-	-	-
STC-GAN[CVPR2018] [22]	7.47	6.93	10.33	0.929	0.947	0.985	27.43	28.67	35.8
SID[ICCV2019] [38]	7.96	7.72	9.64	0.948	0.964	0.986	25.01	26.1	32.88
DSC[TPAMI2019] [39]	6.67	6.39	9.22	0.845	0.885	0.967	26.62	28.18	33.45
RIS-GAN[AAAI2019] [40]	6.62	6.31	9.15	-	-	-	-	-	-
DHAN[AAAI2020] [41]	6.28	5.92	8.43	0.921	0.941	0.983	27.88	29.54	34.79
Auto-Exp[CVPR2021] [42]	5.88	5.51	7.9	0.845	0.879	0.975	27.19	28.6	34.71
<i>Un-Supervised methods</i>									
G2R[CVPR2021] [48]	7.84	7.54	10.71	0.932	0.967	0.974	24.72	26.18	31.62
<i>Half-Supervised learning methods</i>									
Mask-ShadowGAN[2019] [43]	7.63	7.03	10.35	-	-	-	-	-	-
LG-shadow[ECCV2020] [46]	6.67	5.93	11.51	0.906	0.938	0.974	25.83	28.32	31.08
SpA-Former[IJCNN2023] [50]	6.86	6.22	10.48	0.931	0.956	0.982	27.73	30.16	33.51
Our	6.03	5.425	9.72	0.952	0.970	0.986	28.03	30.234	34.44

2) **Rain removal:** As in Table II, and Fig 5, we report the PSNR/SSIM score methods for the rain removal on De-RainDrop testB and testa dataset. Our method is compared with existing methods including CMFNet [57], D-DAM [58], BPP [60], Maxim [61], IDT [59]. Our MemoryNet achieved the best best SSIM score (0.84) and the second best PSNR score (25.38)dB on test-b, the best SSIM score(0.904) and best PSNR(24.64) db on test-a. The figure shows the visualization results of the DeRainDrop test-b image, which well demonstrates that our method effectively removes the raindrops and the recovered image is visually closer to the real image than other models. In order to compare with MMOS [62], a rain removal network that also uses memory module, we also conducted rain removal experiments at MMOS, but the result is realistic that MMOS does not work well on real rain removal datasets, we suppose it may be due to the fact that in real data computation, the use of noisy data is not successfully paired with the pseudo-label generated by the target network.

3) **Image debulrring:** In Table III, and Fig. 6, we report the PSNR/SSIM score methods for the debulrring task. We compare with several very competitive algorithms including Gao [64], DBGAN [65], MT-RNN [66], MPRNet [51] and DGUNet [63], the quantitative evaluation results are presented in Table III, although our MemoryNet does not achieve the best performance, the evaluation score is still satisfied. This means that the proposed model can handle the degradation that occurs, and DGUNet’s results and metrics are by far the best, thanks in large part to its gradient strategy, which they integrate into the gradient descent step of the proximal gradient descent (PGD) algorithm, driving it to handle complex and real-world image degradation.

B. Ablation Study on MemoryNet

Quantitative comparisons on Memory augment

In order to verify the effectiveness of memory augment and comparative learning proposed in this paper, we conducted ablation studies on ISTD datasets, as shown in the Fig. 7 and

Table IV. Because each Memory item calculates the cosine similarity with all queries, and the similarity is completed, we replace our Memory layer, one for three-branches, one for two-branch, and one for single-branch. We conducted ablation experiments to check if it is successful for memory augment, and the Table shows that the memory augment is more suitable for the three-stage recovery network in this research. In order to better visualize the role played by memory proposed in this paper, we performed feature visualization in a lightweight network as shown in Fig. 7, the input is a modal photo, the first layer went through the Memory augment first, and then the convolution layer, as shown in the figure, we can see that the feature map after adding memory is more suitable for network propagation, while the original feature map without adding memory obviously deviates from the original image.

Quantitative comparisons on contrastive learning

Contrastive learning, in contrast to generative learning, does not need to focus on the tedious details of the instances, but only needs to learn to distinguish the data on the feature space at the abstract semantic level, so the model and its optimization become simpler and have greater generalization ability. In this study, we add contrastive learning behind the residual network, transforming it into a discriminator, with the goal of learning an encoder that encodes similar data of the same class while making the encoding results of various classes of data as dissimilar as feasible. As shown in Table IV, the comparative learning in this paper is helpful in a task like de-shadowing and can improve the metrics better. In this paper, combining memory network and contrast learning, it is obvious that PSNR improves by 1 point to 33.44, ssim to 0.986, and RMSE to 6.03.

V. CONCLUSION

In this paper, we propose a general network for image restoration called MemoryNet, it consists of a memory augment and contrastive learning network. It can recover degradation image, including shadows, rain and blur. These three

TABLE II
PERFORMANCE COMPARISON OF RAIN REMOVAL ON RAINDROP(TESTA AND TESTB). THE RED MARKED REPRESENTATIVE RANKED FIRST AND THE BLUE MARKED REPRESENTATIVE RANKED SECOND

Methods	Venue	PSNR-testb	SSIM-testb	PSNR-testa	PSNR-testa
CMFNet [57]	Arxiv 2022	25.51	0.82	24.57	0.898
DeRaindrop [25]	CVPR2018	23.25	0.67	24.23	0.867
D-DAM [58]	Arxiv2021	24.63	0.81	23.71	0.892
BPP [60]	ICIP2021	24.85	0.80	23.93	0.883
MAXIM [61]	CVPR2022	25.74	0.83	-	-
MPRNet [51]	CVPR2021	24.42	0.80	-	-
IDT [59]	PAMI2022	-	-	24.57	0.896
MMOS [62]	CVPR2021	23.816	0.836	-	-
MemoryNet		25.38	0.84	24.64	0.904

TABLE III
PERFORMANCE COMPARISON OF IMAGE DEBULRRING ON GOPRO DATASET). THE RED MARKED REPRESENTATIVE RANKED FIRST AND THE BLUE MARKED REPRESENTATIVE RANKED SECOND

Methods	Venue	PSNR	SSIM
Gao [64]	CVPR2019	29.67	0.928
DBGAN [65]	CVPR2020	29.87	0.935
MT-RNN [66]	ECCV2020	29.92	0.938
MPRNet [51]	CVPR2021	29.97	0.939
DGUNet [63]	CVPR2022	31.48	0.953
MemoryNet		30.76	0.953

experiments demonstrate that these methods are effective in improving restoration performance. In addition, this paper’s model obtains significant PSNR, SSIM gain on three datasets with different degradation types, which is a strong proof that the recovered images are perceptually realistic. In the future, we will try more different recovery tasks, such as image enhancement, stripe removal, etc.

REFERENCES

- [1] Weisheng Dong, Lei Zhang, Guangming Shi, and Xiaolin Wu. Image deblurring and super-resolution by adaptive sparse domain selection and adaptive regularization. TIP, 2011. 1
- [2] Kaiming He, Jian Sun, and Xiaoou Tang. Single image haze removal using dark channel prior. TPAMI, 2010. 1
- [3] Kwang In Kim and Younghee Kwon. Single-image super resolution using sparse regression and natural image prior. TPAMI, 2010. 1
- [4] Pietro Perona and Jitendra Malik. Scale-space and edge detection using anisotropic diffusion. TPAMI, 1990. 1
- [5] Stefan Roth and Michael J Black. Fields of experts: A framework for learning image priors. In CVPR, 2005. 1
- [6] Leonid I Rudin, Stanley Osher, and Emad Fatemi. Nonlinear total variation based noise removal algorithms. Physica D: nonlinear phenomena, 1992. 1, 2
- [7] Song Chun Zhu and David Mumford. Prior learning and gibbs reaction-diffusion. TPAMI, 1997. 1
- [8] Tao Dai, Jianrui Cai, Yongbing Zhang, Shu-Tao Xia, and Lei Zhang. Second-order attention network for single image super-resolution. In CVPR, 2019. 1, 2
- [9] ballero, Andrew Cunningham, Alejandro Acosta, Andrew Aitken, Alykhan Tejani, Johannes Totz, Zehan Wang, et al. Photo-realistic single image super resolution using a generative adversarial network. In CVPR, 2017. 1
- [10] Xingang Pan, Xiaohang Zhan, Bo Dai, Dahua Lin, Chen Change Loy, and Ping Luo. Exploiting deep generative prior for versatile image restoration and manipulation. In ECCV, 2020. 1, 2
- [11] Syed Waqas Zamir, Aditya Arora, Salman Khan, Munawar Hayat, Fahad Shabbaz Khan, Ming-Hsuan Yang, and Ling Shao. CycleISP: Real image restoration via improved data synthesis. In CVPR, 2020. 1, 2, 6, 7, 8
- [12] Hayat, Fahad Shabbaz Khan, Ming-Hsuan Yang, and Ling Shao. Learning enriched features for real image restoration and enhancement. In ECCV, 2020. 1

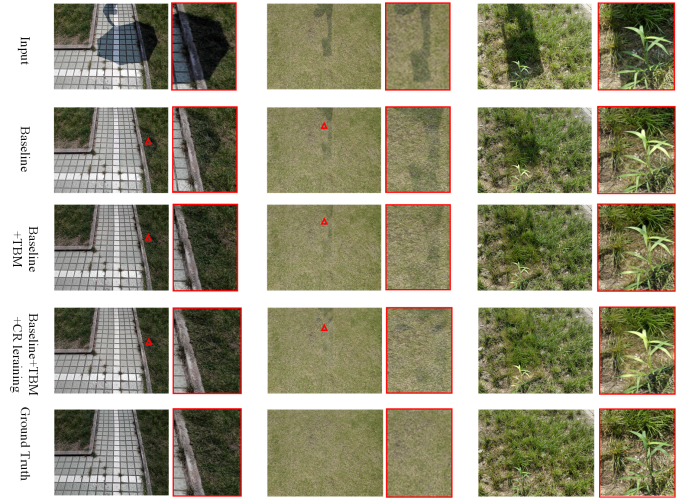


Fig. 7. Feature visualization of memory augment layer, the left is the feature map of the first layer without any processing, and the right is the feature map of the first layer after memory augment

TABLE IV
ABLATION STUDY OF SHADOW REMOVAL ON ISTD DATASET

	RMSE	RMSE-N	RMSE-S	SSIM	PSNR
Baseline	6.74	6.19	10.27	0.921	26.79
Added memory	6.263	5.69	9.763	0.952	27.801
Added Contrastive learning	6.21	5.65	9.58	0.951	27.68
Added memory and Contrastive	6.03	5.425	9.72	0.952	28.023

- [13] Jin Z, Iqbal M Z, Bobkov D, et al. A flexible deep CNN framework for image restoration[J]. IEEE Transactions on Multimedia, 2019, 22(4): 1055-1068.
- [14] Mou C, Zhang J, Fan X, et al. COLA-Net: Collaborative attention network for image restoration[J]. IEEE Transactions on Multimedia, 2021, 24: 1366-1377.
- [15] Ren C, He X, Nguyen T Q. Adjusted non-local regression and directional smoothness for image restoration[J]. IEEE Transactions on Multimedia, 2018, 21(3): 731-745.
- [16] Chang M, Feng H, Xu Z, et al. Low-light image restoration with short- and long-exposure raw pairs[J]. IEEE Transactions on Multimedia, 2021, 24: 702-714.
- [17] Pathak D, Krahenbuhl P, Donahue J, et al. Context encoders: Feature learning by inpainting[C]//Proceedings of the IEEE conference on computer vision and pattern recognition. 2016: 2536-2544.
- [18] Nazeri K, Ng E, Joseph T, et al. Edgeconnect: Generative image inpainting with adversarial edge learning[J]. arXiv preprint [arXiv:1901.00212](https://arxiv.org/abs/1901.00212), 2019.
- [19] Zhang X, Chen F, Wang C, et al. Sienet: Siamese expansion network for image extrapolation[J]. IEEE Signal Processing Letters, 2020, 27: 1590-1594.
- [20] Yan S, Zhang X. PCNet: partial convolution attention mechanism for image inpainting[J]. International Journal of Computers and Applications, 2021: 1-8.
- [21] Zhang X, Wu S, Ding H, et al. Image extrapolation based on multi-column convolutional attention network[C]//2020 IEEE 4th Information Technology, Networking, Electronic and Automation Control Conference (ITNEC). IEEE, 2020, 1: 1938-1942.
- [22] Wang J, Li X, Yang J. Stacked conditional generative adversarial networks for jointly learning shadow detection and shadow removal[C]//Proceedings of the IEEE Conference on Computer Vision and Pattern Recognition. 2018: 1788-1797.
- [23] Qu L, Tian J, He S, et al. Deshadownet: A multi-context embedding deep network for shadow removal[C]//Proceedings of the IEEE Conference on Computer Vision and Pattern Recognition. 2017: 4067-4075.
- [24] Jin Y, Sharma A, Tan R T. DC-ShadowNet: Single-Image Hard and Soft Shadow Removal Using Unsupervised Domain-Classifer Guided Network[C]//Proceedings of the IEEE/CVF International Conference on Computer Vision. 2021: 5027-5036.
- [25] Qian R, Tan R T, Yang W, et al. Attentive generative adversarial network

- for raindrop removal from a single image[C]//Proceedings of the IEEE conference on computer vision and pattern recognition. 2018: 2482-2491.
- [26] Zhang H, Sindagi V, Patel V M. Image de-raining using a conditional generative adversarial network[J]. IEEE transactions on circuits and systems for video technology, 2019, 30(11): 3943-3956.
- [27] Shen R, Zhang X, Xiang Y. AFFNet: attention mechanism network based on fusion feature for image cloud removal[J]. International Journal of Pattern Recognition and Artificial Intelligence, 2022: 2254014.
- [28] Pan H. Cloud removal for remote sensing imagery via spatial attention generative adversarial network[J]. arXiv preprint [arXiv:2009.13015](https://arxiv.org/abs/2009.13015), 2020.
- [29] Li G, He X, Zhang W, et al. Non-locally enhanced encoder-decoder network for single image de-raining[C]//Proceedings of the 26th ACM international conference on Multimedia. 2018: 1056-1064.
- [30] Yang W, Tan R T, Feng J, et al. Deep joint rain detection and removal from a single image[C]//Proceedings of the IEEE conference on computer vision and pattern recognition. 2017: 1357-1366.
- [31] Ren D, Zuo W, Hu Q, et al. Progressive image deraining networks: A better and simpler baseline[C]//Proceedings of the IEEE/CVF Conference on Computer Vision and Pattern Recognition. 2019: 3937-3946.
- [32] Wei W, Meng D, Zhao Q, et al. Semi-supervised transfer learning for image rain removal[C]//Proceedings of the IEEE/CVF conference on computer vision and pattern recognition. 2019: 3877-3886.
- [33] Huang H, Yu A, He R. Memory oriented transfer learning for semi-supervised image deraining[C]//Proceedings of the IEEE/CVF Conference on Computer Vision and Pattern Recognition. 2021: 7732-7741.
- [34] Guo Z K, Hou M, Sima M, et al. DerainAttentionGAN: unsupervised single-image deraining using attention-guided generative adversarial networks[J]. Signal, Image and Video Processing, 2022, 16(1): 185-192.
- [35] R. Guo, Q. Dai, and D. Hoiem, "Paired regions for shadow detection and removal," *IEEE TPAMI*, vol. 35, no. 12, 2012.
- [36] H. Gong and D. Cosker, "Interactive shadow removal and ground truth for variable scene categories," *In Proc. BMVC*, 2014.
- [37] Q. Yang, K. Tan, and N. Ahuja. Shadow removal using bilateral filtering. *IEEE TIP*, 21(10):4361-4368, 2012.
- [38] Le H, Samaras D. Shadow removal via shadow image decomposition[C]//Proceedings of the IEEE/CVF International Conference on Computer Vision. 2019: 8578-8587.
- [39] Hu X, Fu C W, Zhu L, et al. Direction-aware spatial context features for shadow detection and removal[J]. IEEE transactions on pattern analysis and machine intelligence, 2019, 42(11): 2795-2808.
- [40] Zhang L, Long C, Zhang X, et al. Ris-gan: Explore residual and illumination with generative adversarial networks for shadow removal[C]//Proceedings of the AAAI Conference on Artificial Intelligence. 2020, 34(07): 12829-12836.
- [41] Cun X, Pun C M, Shi C. Towards ghost-free shadow removal via dual hierarchical aggregation network and shadow matting GAN[C]//Proceedings of the AAAI Conference on Artificial Intelligence. 2020, 34(07): 10680-10687.
- [42] Fu L, Zhou C, Guo Q, et al. Auto-exposure fusion for single-image shadow removal[C]//Proceedings of the IEEE/CVF Conference on Computer Vision and Pattern Recognition. 2021: 10571-10580.
- [43] Hu X, Jiang Y, Fu C W, et al. Mask-ShadowGAN: Learning to remove shadows from unpaired data[C]//Proceedings of the IEEE/CVF International Conference on Computer Vision. 2019: 2472-2481.
- [44] Chen Z, Long C, Zhang L, et al. CANet: A Context-Aware Network for Shadow Removal[C]//Proceedings of the IEEE/CVF International Conference on Computer Vision. 2021: 4743-4752.
- [45] Hu X, Jiang Y, Fu C W, et al. Mask-ShadowGAN: Learning to remove shadows from unpaired data[C]//Proceedings of the IEEE/CVF International Conference on Computer Vision. 2019: 2472-2481.
- [46] Liu Z, Yin H, Mi Y, et al. Shadow removal by a lightness-guided network with training on unpaired data[J]. IEEE Transactions on Image Processing, 2021, 30: 1853-1865.
- [47] Vasluianu F A, Romero A, Van Gool L, et al. Self-Supervised Shadow Removal[J]. arXiv preprint [arXiv:2010.11619](https://arxiv.org/abs/2010.11619), 2020.
- [48] Liu Z, Yin H, Wu X, et al. From shadow generation to shadow removal[C]//Proceedings of the IEEE/CVF Conference on Computer Vision and Pattern Recognition. 2021: 4927-4936.
- [49] Tan C, Feng X. Unsupervised Shadow Removal Using Target Consistency Generative Adversarial Network[J]. arXiv preprint [arXiv:2010.01291](https://arxiv.org/abs/2010.01291), 2020.
- [50] Zhang X F, Gu C C, Zhu S Y. SpA-Former: Transformer image shadow detection and removal via spatial attention[J]. arXiv e-prints, 2022: arXiv: 2206.10910.
- [51] Zamir S W, Arora A, Khan S, et al. Multi-stage progressive image restoration[C]//Proceedings of the IEEE/CVF conference on computer vision and pattern recognition. 2021: 14821-14831.
- [52] Wu H, Qu Y, Lin S, et al. Contrastive learning for compact single image dehazing[C]//Proceedings of the IEEE/CVF Conference on Computer Vision and Pattern Recognition. 2021: 10551-10560.
- [53] He T, Gong D, Tian Z, et al. Learning and memorizing representative prototypes for 3d point cloud semantic and instance segmentation[C]//European Conference on Computer Vision. Springer, Cham, 2020: 564-580.
- [54] Park H, Noh J, Ham B. Learning memory-guided normality for anomaly detection[C]//Proceedings of the IEEE/CVF Conference on Computer Vision and Pattern Recognition. 2020: 14372-14381.
- [55] Chen F, Wu F, Wu Q, et al. Memory Rectification and Alignment toward Generalizer RGB-Infrared Person[J]. arXiv preprint [arXiv:2109.08843](https://arxiv.org/abs/2109.08843), 2021.
- [56] Gong D, Liu L, Le V, et al. Memorizing normality to detect anomaly: Memory-augmented deep autoencoder for unsupervised anomaly detection[C]//Proceedings of the IEEE/CVF International Conference on Computer Vision. 2019: 1705-1714.
- [57] Fan C M, Liu T J, Liu K H. Compound Multi-branch Feature Fusion for Real Image Restoration[J]. arXiv preprint [arXiv:2206.02748](https://arxiv.org/abs/2206.02748), 2022.
- [58] Zhang K, Li D, Luo W, et al. Dual attention-in-attention model for joint rain streak and raindrop removal[J]. IEEE Transactions on Image Processing, 2021, 30: 7608-7619.
- [59] Xiao J, Fu X, Liu A, et al. Image De-raining Transformer[J]. IEEE Transactions on Pattern Analysis and Machine Intelligence, 2022.
- [60] Pablo Navarrete Michelini, Hanwen Liu, Yunhua Lu, and Xingqun Jiang. Back-Cprojection pipeline. In 2021 IEEE International Conference on Image Processing (ICIP), pp. 1949-C1953. IEEE, 2021.
- [61] Tu Z, Talebi H, Zhang H, et al. Maxim: Multi-axis mlp for image processing[C]//Proceedings of the IEEE/CVF Conference on Computer Vision and Pattern Recognition. 2022: 5769-5780.
- [62] Huang H, Yu A, He R. Memory oriented transfer learning for semi-supervised image deraining[C]//Proceedings of the IEEE/CVF Conference on Computer Vision and Pattern Recognition. 2021: 7732-7741.
- [63] Mou C, Wang Q, Zhang J. Deep Generalized Unfolding Networks for Image Restoration[C]//Proceedings of the IEEE/CVF Conference on Computer Vision and Pattern Recognition. 2022: 17399-17410.
- [64] Hongyun Gao, Xin Tao, Xiaoyong Shen, and Jiaya Jia. Dynamic scene deblurring with parameter selective sharing and nested skip connections. In Proceedings of the IEEE Conference on Computer Vision and Pattern Recognition (CVPR), pages 3848-C3856, 2019. 6, 7
- [65] Stenger, Wei Liu, and Hongdong Li. Deblurring by realistic blurring. In Proceedings of the IEEE Conference on Computer Vision and Pattern Recognition (CVPR), pages 2737-C2746, 2020. 6, 7
- [66] Dongwon Park, Dong Un Kang, Jisoo Kim, and Se Young Chun. Multi-temporal recurrent neural networks for progressive non-uniform single image deblurring with incremental temporal training. In Proceedings of the European Conference on Computer Vision (ECCV), pages 327-C343, 2020. 6, 7
- [67] Seungjun Nah, Tae Hyun Kim, and Kyoung Mu Lee. Deep multi-scale convolutional neural network for dynamic scene deblurring. In Proceedings of the IEEE Conference on Computer Vision and Pattern Recognition (CVPR), pages 3883-C3891, 2017. 6